^{131}I-GD2-ch14.18 Scintigraphy to Evaluate Option for Radioimmunotherapy in Patients with Advanced Tumors

Ying Zhang[1], Juergen Kupferschlaeger[1], Peter Lang[2], Gerald Reischl[3,4], Rupert J. Handgretinger[2], Christian la Fougère[1,4,5], and Helmut Dittmann[1]

[1]*Department of Nuclear Medicine and Clinical Molecular Imaging, University Hospital Tuebingen, Tuebingen, Germany;* [2]*Clinic for Paediatric Hematology and Oncology, University Hospital Tuebingen, Tuebingen, Germany;* [3]*Department of Preclinical Imaging and Radiopharmacy, University Hospital Tuebingen, Tuebingen, Germany;* [4]*Cluster of Excellence iFIT (EXC 2180) "Image Guided and Functionally Instructed Tumor Therapies," University of Tuebingen, Tuebingen, Germany; and* [5]*German Cancer Consortium, Partner Site Tuebingen, Tuebingen, Germany*

The tumor-selective ganglioside antigene GD2 is frequently expressed on neuroblastomas and to a lesser extent on sarcomas and neuroendocrine tumors. The aim of our study was to evaluate the tumor targeting and biodistribution of ^{131}I-labeled chimeric GD2-antibody clone 14/18 (^{131}I-GD2-ch14.18) in patients with late-stage disease in order to identify eligibility for radioimmunotherapy. **Methods:** Twenty patients (neuroblastoma, $n = 9$; sarcoma, $n = 9$; pheochromocytoma, $n = 1$; and neuroendocrine tumor, $n = 1$) were involved in this study. A 21- to 131-MBq dose (1–2 MBq/kg) of ^{131}I-GD2-ch14.18 (0.5–1.0 mg) was injected intravenously. Planar scintigraphy was performed within 1 h from injection (day 0) and on days 1, 2, 3, and 6 or 7 to analyze tumor uptake and tracer biodistribution. Serial blood samples were collected in 4 individuals. Absorbed dose to tumor lesions and organs was calculated using OLINDA software. **Results:** The tumor-targeting rate on a per-patient base was 65% (13/20), with 6 of 9 neuroblastomas showing uptake of ^{131}I-GD2-ch14.18. Tumor lesions showed maximum uptake at 20–64 h after injection (effective half-life in tumors, 33–192 h). The tumor-absorbed dose varied between 0.52 and 30.2 mGy/MBq (median, 9.08 mGy/MBq; $n = 13$). Visual analysis showed prominent blood-pool activity up to day 2 or 3 after injection. No pronounced uptake was observed in the bone marrow compartment or in the kidneys. Bone marrow dose was calculated at 0.09–0.18 mGy/MBq (median, 0.12 mGy/MBq), whereas blood dose was 1.1–4.7 mGy/MBq. Two patients (1 neuroblastoma and 1 pheochromocytoma) with particularly high tumor uptake underwent radioimmunotherapy using 2.3 and 2.9 GBq of ^{131}I-GD2-ch14.18, both achieving stable disease. Overall survival was 17 and 6 mo, respectively. **Conclusion:** ^{131}I-GD2-ch14.18 is cleared slowly from blood, not resulting in good tumor-to-background contrast until 2 d after application. With acceptable red marrow and organ dose, radioimmunotherapy is an option for patients with high tumor uptake. However, because of the variable GD2 expression, the decision should depend on pretherapeutic dosimetry.

Key Words: ^{131}I-GD2; neuroblastoma; dosimetry; tumor dose; radioimmunotherapy

J Nucl Med 2022; 63:205–211
DOI: 10.2967/jnumed.120.261854

Received Dec. 17, 2020; revision accepted Apr. 21, 2021.
For correspondence or reprints, contact: Ying Zhang (ying.zhang@med.uni-tuebingen.de).
Published online May 28, 2021.

The disialoganglioside GD2 is a sialic acid–containing glycosphingolipid physiologically expressed on cell surfaces in the central nervous system, peripheral sensory nerve fibers, and skin melanocytes at low levels (*1–3*). High GD2 expression has been recognized in tumors such as neuroblastoma, in bone and soft-tissue sarcoma, in neuroendocrine tumors, and in some brain tumors (*1*,*4*). Antibodies targeting GD2 have been shown to exert antibody-dependent and complement-dependent cytotoxicity in tumor cells (*1*,*5*,*6*). For tumor-specific therapy, the chimeric antibody dinutuximab (ch14.18) received approval for an orphan drug designation in 2015 from the U.S. Food and Drug Administration at a dose of 17.5 mg/m^2/d. It is the first monoclonal antibody specifically approved for maintenance treatment of pediatric patients with high-risk neuroblastoma who have achieved at least a partial response to first-line multimodal therapy. In patients with neuroblastoma, dinutuximab was shown to increase the 2-y event-free survival rate from approximately 46% with standard treatment to 66% (*6–8*). Similar to this result, some patients with refractory or recurrent disease achieved benefit from an anti-GD2 therapy (*9–11*).

Radioimmunotherapy also involves selective targeting of cancer-associated cell antigens, primarily using the antibody as a carrier vehicle for radionuclides that deliver irradiation to tumor areas (*12*). Thus, the anticancer activity of radioimmunotherapy is predominantly due to irradiation rather than antibody- or complement-dependent cytotoxicity. As a result, radiation-sensitive tumors such as leukemia and lymphomas are good candidates for radioimmunotherapy. In particular, CD20-targeted radioimmunotherapy using ^{131}I (^{131}I-tositumomab) (*13*) and ^{90}Y-labeled antibodies (^{90}Y-ibritumomab tiuxetan) (*14*) have demonstrated durable remission of B-cell lymphoma. GD2-targeting radioimmunotherapy in high-risk neuroblastoma patients was first evaluated using the murine antibody 3F8 labeled with ^{131}I (*15*). In the subgroup of patient receiving ^{131}I-3F8, the engraftment of autologous bone marrow transplantation was successful, and long-term progression-free survival was comparable to a combination therapy with 3F8 and granulocyte-macrophage colony-stimulating factor for patients in a first complete response (*16*).

Accurate patient stratification is of the upmost interest, and there are several criteria that might help to identify eligibility for radioimmunotherapy (*12*). Besides tumor specificity and high target antigen expression, low uptake of the radiolabeled antibody in organs such as the liver, spleen, and kidneys is crucial (*17*).

Thus, evaluation of in vivo biodistribution is a key step toward considering new applications of radioimmunotherapy (*18*).

For immunotherapies such as dinutuximab, with regard to potential adverse effects—for example, neuropathic pain, infusion reactions such as hypersensitivity, hypotension, and occasionally capillary leak syndrome (*7*,*19*)—it is highly desirable to identify eligibility (for immunotherapy and radioimmunotherapy) before making a decision about further treatment. Therefore, the aim of this pilot study was to evaluate the tumor targeting and biodistribution of the ^{131}I-labeled GD2-antibody ch14.18 (^{131}I-GD2-ch14.18) in patients with late-stage disease and ultimately identify candidates for radioimmunotherapy.

MATERIALS AND METHODS

Antibody Preparation and Radiolabeling

^{131}I for labeling in sodium hydroxide solution was purchased from GE Healthcare Buchler. The antibody GD2-mAb (ch14.18) in sterile aqueous solution (~4–5 mg/mL) was provided by the children's hospital of our institution in a quality suitable for clinical trials. As an iodination reagent, Iodo-Gen (Thermo Fisher Scientific) was used. All other chemicals and materials were provided by commercial suppliers. According to supplier instructions, 200 μL of a solution (1 mg/mL) of Iodo-Gen in CH_2Cl_2 were introduced per vial, followed by evaporation at room temperature. Coated vials were stored for a maximum of 1 wk under inert gas in the dark.

For diagnostic application, 1–2 mg of antibody (200–400 μL of antibody solution) were added to a coated vial, followed by the acquired amount of ^{131}I (25–100 μL) corresponding to 50–175 MBq. For therapeutic application, 5 mg of GD2-ch14.18 and 3,000–4,000 MBq of ^{131}I were used for the otherwise identical labeling procedure.

Patients and Clinical Characteristics

The need for written informed consent for this study was waived by the institutional review board (registry 821/2020BO2). Following the stipulations of the German medicinal products act ("Arzneimittelgesetz"; AMG §13[2b]), ^{131}I-GD2-ch14.18 was used in patients with late-stage disease and in order to identify candidates for radioimmunotherapy.

In total, 20 patients were included in this retrospective analysis (Table 1). All patients had a history of surgical tumor resection and systemic chemotherapy. Neuroblastoma patients (8 children and 1 adult) had stage IV disease and had previously been treated by myeloablative chemotherapy with autologous hematopoietic stem cell rescue. Four of 9 patients additionally received external-beam irradiation, and 5 of 9 received nonradioactive GD2-antibody therapy. All neuroblastoma patients underwent ^{123}I-metaiodobenzylguanidine (^{123}I-MIBG) scintigraphy, which demonstrated tumor uptake in only 3 of 9 cases. Individuals with ^{123}I-MIBG–positive tumors had earlier received ^{131}I-MIBG therapy. Patients with metastatic sarcoma were predominantly adults ($n = 6/9$; age range, 18–51 y). One of the remaining 2 patients had advanced neuroendocrine tumor, and the other had malignant pheochromocytoma. MRI or CT imaging was used as the reference standard for detection of tumor manifestations on ^{131}I-GD2-ch14.18 scans.

Protocol for Scintigraphy

A 21- to 131-MBq dose (1–3 MBq/kg) of ^{131}I-GD2-ch14.18 (0.5–1.0 mg of antibody) was diluted in 100 mL of 0.9% NaCl and infused intravenously over 45–60 min. Premedication included antihistamines and prednisolone. Whole-body (WB) planar scintigraphy was performed using a double-head γ-camera (Hawkeye/Millenium VG; GE Healthcare) with a high-energy general-purpose collimator and a matrix size of 1,024 × 256 pixels. The energy window was set at 364 ± 36 keV for ^{131}I. Acquisitions were performed at 1, 24, 48, and 72 h after injection, as well as, if possible, 5–6 d after injection. Additional SPECT/CT of tumor regions was performed for some patients. Serial blood samples were collected from 4 patients (3 adults and 1 child).

^{131}I-GD2-ch14.18 Treatment

Two adult patients (1 neuroblastoma and 1 pheochromocytoma) received treatment with ^{131}I-GD2-ch14.18 (2,275 MBq with 1.7 mg of GD2-Ab and 2,942 MBq with 1.6 mg of GD2-Ab, respectively). Comedications included dexamethasone, 8 mg to 16 mg daily for 5 d; antihistamines; and analgesia, if required. The patients were hospitalized for 4–5 d after the infusion. Posttreatment evaluations included clinical status, vital signs, neurologic examination, blood for serum chemistries, and electrocardiography. The hemogram was checked 0.5, 1, 2, and 3 mo after treatment. WB CT imaging was performed 2 and 5 mo after treatment.

Normalized Blood Tracer Concentration

Activity concentrations (Bq/mL) from blood samples (0.1–0.5 mL of full blood) were determined using an automatic γ-counter (Wizard 1480; Wallac). Data were corrected for background radiation, cross over, dead time, and decay due to the collection times of the individual samples. A final normalization of the injected activity was calculated with the normalized blood tracer concentration and expressed as percentage injected activity per milliliter.

Biodistribution

Distribution of radioactivity in various organs was measured using count rates in regions of interest defined on serial planar scans. A baseline scan was performed within 1 h from activity infusion before the first urination. Data were expressed as percentage WB count fraction of injected activity.

Since data from 1 patient were not eligible for biodistribution measurement, the statistics were based on 19 patients. Time–activity curves were drawn for visually well-defined GD2-positive tumors (fraction of injected activity per cubic centimeter of tumor, $n = 12$ patients).

Bone Marrow Dose

The bone marrow dose was calculated using the following equation (20):

$$\text{Bone marrow dose}\left[\frac{\text{mGy}}{\text{MBq}}\right] = 0.058\times\tilde{A}_{\text{blood}}\times m_{\text{RM}} \times\frac{\text{RMECFF}}{(1-\text{HCT})\times A_{\text{injected}}}$$

where A_{blood} denotes the accumulated blood activity concentration (MBq × h/g), m_{RM} denotes the mass of red bone marrow (g), and A_{injected} denotes the injected activity (MBq). RMECFF is red marrow extracellular fluid fraction, and HCT denotes hematocrit.

The red bone marrow mass was calculated from the total body weight (g) multiplied by 1.37% in male patients and 1.16% in female patients (*21*). The dose conversion factor RMECFF/(1 − HCT) was assumed to be 0.32 (*20*).

Dosimetry

Radiation doses absorbed by WB, heart, lung, liver, spleen, and kidney were calculated from the ^{131}I time-integrated activity coefficient (TIAC) in the defined region of interest. Organ radioactivity content was estimated from the geometric mean of anterior and posterior region-of-interest counts. A standard marker of ^{131}I-GD2-ch14.18 (~1 MBq) was placed in each WB scan as a reference to ensure constancy of γ-camera electronics and scan speed. These data were fitted to a rising and falling exponential function:

$$Y(t) = A[1-\exp(-\alpha t)]\cdot\exp(-\beta t)$$

Integration of the equation for $Y(t)$ yields the cumulative activity in counts × h (or fraction of injected activity × h). Finally, OLINDA

TABLE 1
Patient Characteristics, ^{131}I-GD2-ch14.18 Activity, and Tumor Detectability on GD2 Scans

Patient no.	Sex	Age (y)	BMI	Histology	Prior treatments	Histology and MIBG scan	Tumor sites	Activity (MBq)	Tumor detection
1	M	23	21	Neuroblastoma	S, chemo, RT	G3, MIBG neg	Bone, hep, lym	82.3	Pos
2	M	32	23	Pheochromocytoma	S, chemo, RT, PRRT	Chromogranine pos	Bone, hep, pul	89.7	Pos
3	F	50	21	Neuroendocrine tumor	Chemo, RT	Chromogranine pos	Bone, hep, lym, pul	87.2	Pos
4	M	7	13	Neuroblastoma	S, chemo, RT, ABMT	MIBG neg, VMA/HVA neg, MYCN pos	Bone	50.8	Pos
5	F	8	16	Neuroblastoma	S, chemo, RT, ABMT	MIBG, NSE, VMA, MYCN neg	Bone, BM	32.6	Pos
6	M	8	16	Neuroblastoma	S, chemo, RT, ABMT	MYCN neg, no chromosome aberration 1 (p36)	Bone	27	Pos
7*	M	7	14	Neuroblastoma	S, chemo, RT, ABMT, GD2	MYCN neg, MIBG pos	Bone, BM	24.7	Neg
8*	M	4	16	Neuroblastoma	S, chemo, MIBG-T, ABMT	MYCN neg, imbalance chromosome 1 (p36)	Bone, BM	21.2	Neg
9	F	4	13	Neuroblastoma	S, chemo, RT, ABMT	MIBG neg	Bone, lym	22.3	Pos
10	F	13	15	Neuroblastoma	S, chemo, MIBG-T, ABMT, GD2	MYCN neg, 1 p-deletion pos, catecholamine pos, MIBG pos	Bone, BM	46.8	Pos
11	M	51	29	Ewing sarcina	S, chemo, RT, ABMT	Ewing sarcoma	Cerebral, pul	83.2	Neg
12	F	20	19	Ewing sarcina	S, chemo, RT, ABMT	Ewing sarcoma	Hep, pul	59	Neg
13	M	18	30	Ewing sarcina	S, chemo	Ewing sarcoma	Pul	130.8	Neg
14	M	13	25	Ewing sarcina	S, chemo, RT, ABMT	Ewing sarcoma	Bone, pul	76.5	Pos
15	M	17	18	Ewing sarcina	S, chemo, ABMT	Ewing sarcoma	Bone, lym	80.5	Pos
16	F	18	27	Ewing sarcina	S, chemo, RT, ABMT	Ewing sarcoma	Bone	79.5	Pos
17	M	19	19	Osteosarcoma	S, chemo	Osteosarcoma	Bone, lym, pul, soft	82.1	Pos
18	M	11	19	Osteosarcoma	S, GD2	Osteosarcoma	No metastasis	84	Pos
19	M	22	17	Osteosarcoma	S, chemo	Osteosarcoma	GI, pul	105	Neg
20*	M	5	17	Neuroblastoma	S, chemo, RT, ABMT	MYCN and MIBG neg, no chromosome aberration 1 (p36)	Bone, BM, lym	59.3	Neg

*Not suitable for dosimetric analysis.

BMI = body mass index; MIBG-T = ^{131}I-MIBG therapy; S = surgery; chemo = chemotherapy; RT = focal radiotherapy; neg = negative; bone = skeletal metastases; hep = hepatic metastases; lym = lymph node metastases; pos = positive; PRRT = peptide receptor radiotherapy; pul = pulmonary metastases; ABMT = myeloablative chemotherapy with stem-cell rescue; VMA = vanillylmandelic acid; HVA = homovanillic acid; MYCN = N-myc proto-oncogene protein; NSE = neuron-specific enolase; BM = bone marrow metastases; GD2 = nonradioactive GD2-antibody therapy; soft = soft-tissue metastases; GI = gastrointestinal tract metastases.

software (Vanderbilt University) was used for dosimetric analysis of all patients.

Tumor Uptake and Tumor TIACs

Absorbed doses of tumors were calculated from regions of interest, with background correction and tumor volumes measured from CT or MRT scans. In patients presenting with multiple tumor lesions, a reference tumor site was defined on the basis of the CT or MRI data comprising the best-delineated or largest lesion. Because time–activity curves showed increasing uptake in tumor regions during the examination cycle, the above equation could not be applied for tumor TIAC. For this reason, we used the following formulas for TIAC in tumor regions:

$$\tau_{\text{tumor}} = \tilde{A}_{\text{tumor}}/A_{\text{injected}}$$

and

$$\tilde{A}_{\text{tumor}} = \int_0^{\infty} dt\ A(t) = \int_0^{T} dt\ A(t) + \int_T^{\infty} dt\ A(t)$$

where the first integral was approximated from experimental data using the trapezoidal rule and the second integral was analytically solved using the last measured value and a monoexponential decay with physical half-life time.

Statistics

Results are shown as means ± SDs. Data were calculated using Microsoft Excel software. Statistical testing (1-way ANOVA) was performed using SigmaStat software (version 3.5; Systat Software). For analyzing the significance of the results, a *t* test based on range was used. A *P* of less than 0.05 was regarded as significant.

RESULTS

Biodistribution

Application of ^{131}I-GD2-ch14.18 was accompanied by a sensation of mild to moderate malaise and tightness in the chest during infusion in most patients (18/20). In addition, grade 3 generalized pain was observed in 2 patients (patients 3 and 17). These side effects were completely resolved right after the end of infusion in all cases. All patients underwent a sequential WB scintigraphy scan up to day 4. Data from 3 patients were not sufficient for dosimetry—in one (patient 7), because of a missing scan on day 1, and in two (patients 8 and 20), because there were only 2 consecutive scans. Thus, scans from 17 individuals were used for dosimetric analyses. The tumor-targeting rate on a per-patient base was 65% (13/20). In particular, 6 of 9 investigated patients with neuroblastoma showed uptake of ^{131}I-GD2-ch14.18. Clinical characteristics and tumor detectability on GD2 scans are depicted in Table 1. The liver and spleen were visualized in all patients, except for one with a history of splenectomy. The urinary bladder showed pronounced radioactivity in most patients, usually on days 1 and 2. No remarkable uptake was seen in the bone marrow compartment or in the kidneys at any time point.

The blood activity concentration in 3 adults indicated nearly complete retention of ^{131}I-GD2-ch14.18 in the blood compartment up to 2 h after infusion (0.0174% ± 0.0018% injected activity/mL at 0.1 h after injection), followed by a decrease with an effective blood half-life of approximately 24 h (Fig. 1A). Data from a single pediatric patient (Fig. 1B) showed a higher blood activity right after the tracer application (0.053% injected activity/mL) and an effective blood half-life of 41 h.

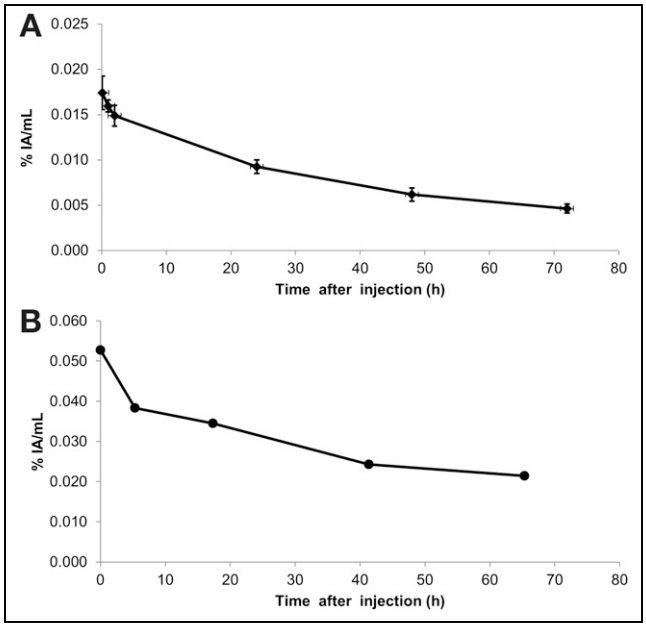

FIGURE 1. Normalized blood tracer concentrations at different time points (percentage injected activity [IA] of ^{131}I-GD2-ch14.18 per milliliter of blood). (A) Mean ± SD from 3 adults (patients 1–3). (B) Values from 1 pediatric patient (6-y-old boy, patient 4).

A typical example of sequential planar WB scans is depicted in Figure 2. Analysis of biodistribution (Fig. 3) demonstrated that the activity of ^{131}I-GD2-ch14.18 in organs peaked within the first hour and continually declined thereafter (lung, 8.02% ± 1.17%; liver, 9.33% ± 1.63%; spleen, 2.07% ± 0.64%; and kidney, 2.24% ± 0.91%, at 1 h after injection, vs. lung, 5.20% ± 1.24%; liver, 5.39% ± 1.42%; spleen, 1.25% ± 0.42%; and kidney, 1.21% ± 0.61%, at 24 h after injection). Tumor lesions showed uptake in 13 of 20 patients, but a sole pelvic tumor lesion in patient 16 was partly superimposed by the urinary bladder. Hence, tumor dosimetry could be performed for 12 patients.

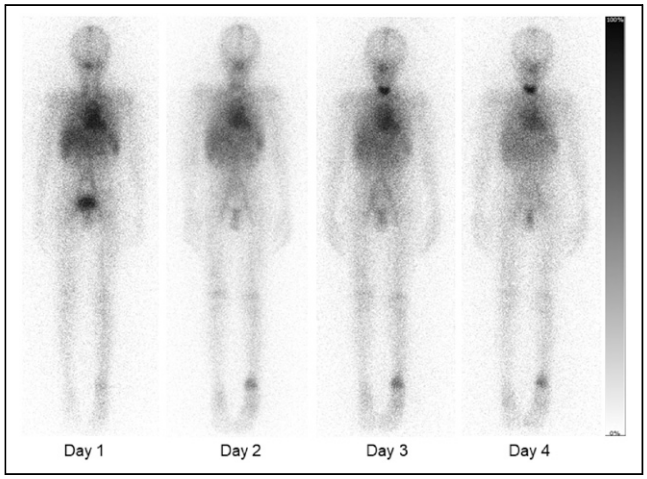

FIGURE 2. Sequential planar WB ^{131}I-GD2-ch14.18 scans (anterior view) demonstrating increased targeting of tumor lesion in left distal tibia on days 2–4 in patient 18, with osteosarcoma.

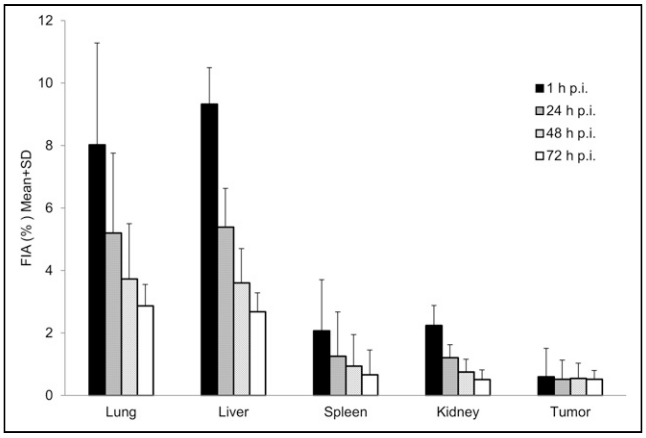

FIGURE 3. Biodistribution as calculated from region-of-interest analysis of planar scintigraphy (n = 19). ^{131}I-GD2-ch14.18 uptake in organ and tumor lesions is expressed as fraction of injected activity (FIA) (mean ± SD) at different time points after injection (p.i.).

In contrast, GD2-expressing tumors showed no early peak but a more stable activity level, with maximum uptake between 1 and 3 d after injection (0.60% ± 0.85% at 1 h after injection, 0.52% ± 0.65% at 24 h after injection, 0.54% ± 0.69% at 48 h after injection, and 0.52% ± 0.63% at 72 h after injection) (Fig. 3). Of note, the tumoral activity varied over a wide range between individuals (Fig. 4). Because of the high blood-pool activity level on early scans, tumor-to-background contrast was best on day 2 or later.

Dosimetry

Quantification of the absorbed radiation dose is presented in Table 2. The calculated median and mean doses to tumor lesions were 9.08 and 11.83 mGy/MBq, respectively. The ratios of median tumor-to-organ doses were 10.32 for lungs, 15.93 for liver, 7.90 for spleen, 15.93 for kidneys, and 75.67 for red bone marrow. The individual absorbed tumor dose varied over a range between 0.52 and 30.20 mGy/MBq. The noticeably highest and lowest values were both from Ewing sarcoma patients. All 6 GD2-positive neuroblastoma patients showed intense uptake, with a median tumor dose of 8.50 mGy/MBq.

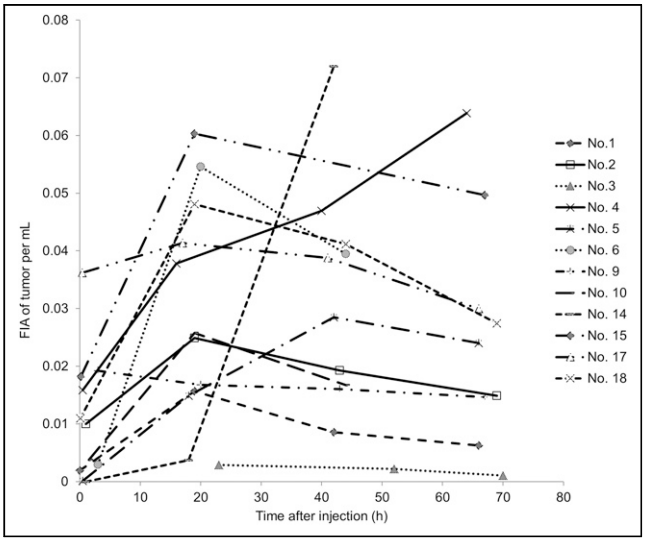

FIGURE 4. Time–activity curves for GD2-positive tumors (fraction of injected activity [FIA] of tumor volume per cubic centimeter). Data represent uptake of reference tumor lesions in 12 patients. Because of overlapping of tumor lesion with urinary bladder, patient 16 was excluded.

TABLE 2
^{131}I-GD2-ch14.18 Absorbed Dose (mGy/MBq)

Target organ	Median	Minimum	Maximum	n	Mean	SD
Red marrow	0.12	0.09	0.18	4	0.12	0.03
Lung	0.88	0.29	3.31	17	1.20	0.86
Liver	0.57	0.23	1.70	17	0.70	0.41
Spleen	1.15	0.40	4.41	16	1.51	1.13
Kidney	0.57	0.19	1.89	17	0.72	0.48
Total body	0.30	0.09	1.46	17	0.41	0.34
Tumor	9.08	0.52	30.20	12	11.83	8.10
Effective dose	0.43	0.12	2.68	17	0.61	0.59

Radioimmunotherapy

Two adult patients (patient 1, with neuroblastoma, and patient 2, with pheochromocytoma) who showed intense tumor uptake (tumor dose, 6.7 and 8.2 mGy/MBq) were selected to receive radioimmunotherapy with I-GD2-ch14.18. The bone marrow dose was calculated at 0.11 and 0.18 mGy/MBq, respectively. An activity of 2.3 and 2.9 GBq (30–40 MBq/kg) of I-GD2-ch14.18 was applied for radioimmunotherapy. Treatment was well tolerated in both cases. Both patients received posttherapeutic imaging with WB scans and additional SPECT/CT. Figure 5 depicts intense targeting of bone and liver tumor lesions in the patient with neuroblastoma on day 2 after radioimmunotherapy.

Follow-up imaging after 2 mo (CT or MRI) showed stable disease with metastases in the patient with neuroblastoma. Moderate thrombocytopenia was observed in this patient 4 wk after radioimmunotherapy and spontaneously recovered after another 4 wk. However, the patient with pheochromocytoma presented with progression of metastases in the bone, bone marrow, liver, and lung 2 mo after radioimmunotherapy. Pancytopenia with severe thrombocytopenia (19,000/μL) occurred in this patient 6 wk after radioimmunotherapy. The improvement thereafter indicates that the radioimmunotherapy was the possible cause. Underlying limited hematopoiesis due to heavy pretreatment, as well as bone marrow tumor involvement, were likely cofactors. The overall survival of these patients was 17 and 6 mo from radioimmunotherapy, respectively.

DISCUSSION

Even though radionuclide therapies such as MIBG or peptide receptor radionuclide therapy are readily available for neuroblastoma or neuroendocrine tumor, patients with insufficient targeting or refractory disease may be candidates for GD2-directed radioimmunotherapy. Immunotherapy targeting GD2 using the chimeric antibody ch14.18 has been studied extensively, but its use as a radiolabeled compound and thus dosimetry in humans as a prerequisite for radioimmunotherapy have been lacking so far. Our results confirmed significant GD2 targeting in most tumors investigated. In particular, most patients with advanced neuroblastoma showed intense tumor uptake. These results correspond to the

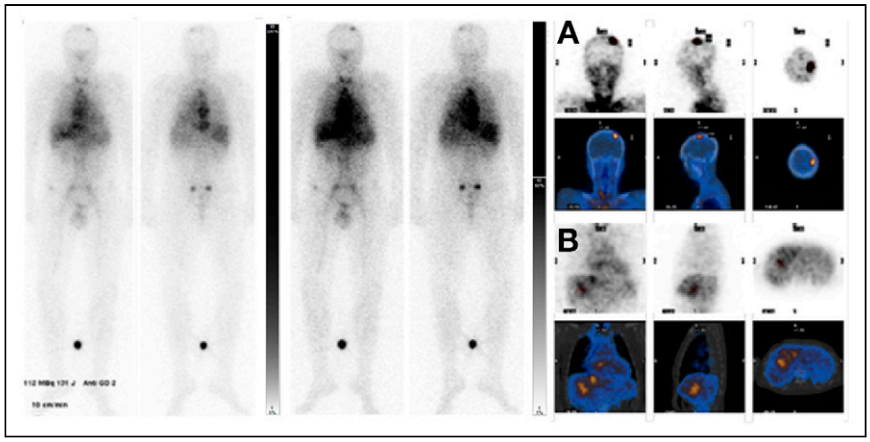

FIGURE 5. ^{131}I-GD2-ch14.18 scan (left) with additional SPECT/CT on day 2 from application demonstrates intense targeting of bone (A) and liver (B) tumor lesions in patient 1, with neuroblastoma.

findings of Reuland et al. (*22*), who revealed GD2 targeting in a cohort of largely MIBG-negative neuroblastomas using the same antibody but labeled with ^{99m}Tc. GD2 targeting was currently also demonstrated in 2 individuals with osteosarcoma and 3 of 6 patients with Ewing sarcomas, as is in line with the variable expression of the target antigen in these malignancies (*23*). Overall, our study revealed that the ch14.18 antibody retains its antigen-binding ability after labeling with ^{131}I.

Serial WB scans showed a slow but continuous decline of organ and blood radioactivity, whereas GD2-positive tumor lesions demonstrated relatively stable radiotracer retention over time. This resulted in good tumor-to-background contrast from 2 d after tracer injection. Slow clearance of radioactivity from the blood is common for radiopharmaceuticals based on full-size monoclonal antibodies (*24*) and has in fact been observed previously with ^{64}Cu-labeled GD2-ch14.18 antibody in an animal model (*25*,*26*). The prolonged blood residence of the antibody conjugate will contribute to absorbed dose in blood-bearing organs such as the liver, spleen, heart, kidneys, and bone marrow. Nevertheless, dosimetry in GD2-positive tumors revealed 10-fold higher or even better tumor-to-organ dose ratios—that is, therapeutic indices—thus meeting published criteria for radioimmunotherapy (*12*).

Despite premedication, mild to moderate antigen reactions were observed under infusion of I-GD2-ch14.18 in most of our patients, whereas 2 individuals additionally experienced diffuse pain. Such antigen toxicity is well known from therapeutic application of nonradioactive GD2-targeting antibodies (*27*) and has been shown to be dose-dependent (*28*). However, the amount of antibody injected for scintigraphy (maximum, 1 mg) was less than 10% of the approved dose in nonradioactive immunotherapy with dinutuximab.

Our study had some limitations. Only planar scintigraphy was available for sequential imaging, and SPECT/CT was added in only selected cases, aiming to better delineate tumor sites. As a result, dose estimations are based on planar scans alone and have to be considered merely semiquantitative, as the combined uncertainties are considered a factor of 2 or even greater (*29*). Moreover, overlap of lesions and blood pool or organs may prevent precise identification of tumor lesions. A dual integral formula was used to estimate tumor TIAC. Because effective half-life after the last measured time point was unknown, physical decay was used for the second integral. As a result, the true tumor-absorbed dose might be considerably lower. Obviously, an elaborate dosimetry will be needed for volume-of-interest analyses using quantitative SPECT/CT (*30*) or PET/CT (*25*). Serial blood samples were available for only 4 of 20 patients; thus, analyses of ^{131}I-GD2-ch14.18 blood kinetics and red marrow dose are to be regarded as preliminary. Finally, because of the small number of patients in this retrospective analysis, tumor targeting and, especially, the safety and efficacy of ^{131}I-GD2-ch14.18 radioimmunotherapy will have to be further evaluated in prospective studies.

CONCLUSION

Sequential scintigraphy demonstrated slow clearance of ^{131}I-GD2-ch14.18 from blood, resulting in favorable tumor-to-background contrast from 2 d after application. With an acceptable red marrow dose, radioimmunotherapy may be considered an option for patients with high tumor uptake. Because of the variable GD2 expression, pretherapeutic imaging and dosimetry are recommended. Development of GD2-targeting fragments might accelerate blood clearance and may improve radioimmunotherapy in the future.

DISCLOSURE

This work was funded by the Deutsche Forschungsgemeinschaft (DFG, German Research Foundation) under Germany's Excellence Strategy (EXC 2180-390900677). No other potential conflict of interest relevant to this article was reported.

KEY POINTS

QUESTION: What are the tumor targeting and biodistribution of ^{131}I-GD2-ch14.18 in patients with late-stage disease who are potentially eligible for radioimmunotherapy?

PERTINENT FINDINGS: In this retrospective study, sequential scintigraphy demonstrated a favorable tumor-to-background contrast for ^{131}I-GD2-ch14.18 from 2 d after application. Moreover, dosimetry in planar scintigraphy in GD2-positive tumors revealed up to 10-fold higher tumor-to-organ dose ratios—that is, therapeutic indices.

IMPLICATIONS FOR PATIENT CARE: With an acceptable red marrow dose, radioimmunotherapy may be an option for patients with high tumor uptake. Because of the variable GD2 expression, pretherapeutic imaging and dosimetry are recommended.

REFERENCES

1. Mujoo K, Cheresh DA, Yang HM, Reisfeld RA. Disialoganglioside GD2 on human neuroblastoma cells: target antigen for monoclonal antibody-mediated cytolysis and suppression of tumor growth. *Cancer Res.* 1987;47:1098–1104.
2. Schulz G, Cheresh DA, Varki NM, Yu A, Staffileno LK, Reisfeld RA. Detection of ganglioside GD2 in tumor tissues and sera of neuroblastoma patients. *Cancer Res.* 1984;44:5914–5920.
3. Svennerholm L, Bostrom K, Fredman P, et al. Gangliosides and allied glycosphingolipids in human peripheral nerve and spinal cord. *Biochim Biophys Acta.* 1994; 1214:115–123.

4. Chang HR, Cordon-Cardo C, Houghton AN, Cheung NK, Brennan MF. Expression of disialogangliosides GD2 and GD3 on human soft tissue sarcomas. *Cancer.* 1992;70:633–638.
5. Navid F, Santana VM, Barfield RC. Anti-GD2 antibody therapy for GD2-expressing tumors. *Curr Cancer Drug Targets.* 2010;10:200–209.
6. Ploessl C, Pan A, Maples KT, Lowe DK. Dinutuximab: an anti-GD2 monoclonal antibody for high-risk neuroblastoma. *Ann Pharmacother.* 2016;50:416–422.
7. Ladenstein R, Potschger U, Valteau-Couanet D, et al. Interleukin 2 with anti-GD2 antibody ch14.18/CHO (dinutuximab beta) in patients with high-risk neuroblastoma (HR-NBL1/SIOPEN): a multicentre, randomised, phase 3 trial. *Lancet Oncol.* 2018;19:1617–1629.
8. Yu AL, Gilman AL, Ozkaynak MF, et al. Anti-GD2 antibody with GM-CSF, interleukin-2, and isotretinoin for neuroblastoma. *N Engl J Med.* 2010;363:1324–1334.
9. Dinutuximab approved for high-risk neuroblastoma. *Cancer Discov.* 2015;5:OF5.
10. Ehlert K, Hansjuergens I, Zinke A, et al. Nivolumab and dinutuximab beta in two patients with refractory neuroblastoma. *J Immunother Cancer.* 2020;8:e00540.
11. Gohil K. Pharmaceutical approval update. *P&T.* 2015;40:327–360.
12. Larson SM, Carrasquillo JA, Cheung NK, Press OW. Radioimmunotherapy of human tumours. *Nat Rev Cancer.* 2015;15:347–360.
13. Kaminski MS, Zelenetz AD, Press OW, et al. Pivotal study of iodine I 131 tositumomab for chemotherapy-refractory low-grade or transformed low-grade B-cell non-Hodgkin's lymphomas. *J Clin Oncol.* 2001;19:3918–3928.
14. Witzig TE, Gordon LI, Cabanillas F, et al. Randomized controlled trial of yttrium-90-labeled ibritumomab tiuxetan radioimmunotherapy versus rituximab immunotherapy for patients with relapsed or refractory low-grade, follicular, or transformed B-cell non-Hodgkin's lymphoma. *J Clin Oncol.* 2002;20:2453–2463.
15. Cheung NK, Kushner BH, LaQuaglia M, et al. N7: a novel multi-modality therapy of high risk neuroblastoma (NB) in children diagnosed over 1 year of age. *Med Pediatr Oncol.* 2001;36:227–230.
16. Cheung NK, Cheung IY, Kushner BH, et al. Murine anti-GD2 monoclonal antibody 3F8 combined with granulocyte-macrophage colony-stimulating factor and 13-cis-retinoic acid in high-risk patients with stage 4 neuroblastoma in first remission. *J Clin Oncol.* 2012;30:3264–3270.
17. Maxon HR, Thomas SR, Hertzberg VS, et al. Relation between effective radiation dose and outcome of radioiodine therapy for thyroid cancer. *N Engl J Med.* 1983;309:937–941.
18. Press OW, Eary JF, Appelbaum FR, et al. Radiolabeled-antibody therapy of B-cell lymphoma with autologous bone marrow support. *N Engl J Med.* 1993;329:1219–1224.
19. Ozkaynak MF, Gilman AL, London WB, et al. A comprehensive safety trial of chimeric antibody 14.18 with GM-CSF, IL-2, and isotretinoin in high-risk neuroblastoma patients following myeloablative therapy: Children's Oncology Group study ANBL0931. *Front Immunol.* 2018;9:1355.
20. Stabin MG, Siegel JA, Sparks RB. Sensitivity of model-based calculations of red marrow dosimetry to changes in patient-specific parameters. *Cancer Biother Radiopharm.* 2002;17:535–543.
21. Woodard HQ. The relation of weight of haematopoietic marrow to body weight. *Br J Radiol.* 1984;57:903–907.
22. Reuland P, Geiger L, Thelen MH, et al. Follow-up in neuroblastoma: comparison of metaiodobenzylguanidine and a chimeric anti-GD2 antibody for detection of tumor relapse and therapy response. *J Pediatr Hematol Oncol.* 2001;23:437–442.
23. Dobrenkov K, Ostrovnaya I, Gu J, Cheung IY, Cheung NK. Oncotargets GD2 and GD3 are highly expressed in sarcomas of children, adolescents, and young adults. *Pediatr Blood Cancer.* 2016;63:1780–1785.
24. Lewis MR, Wang M, Axworthy DB, et al. In vivo evaluation of pretargeted ^{64}Cu for tumor imaging and therapy. *J Nucl Med.* 2003;44:1284–1292.
25. Dearling JL, Voss SD, Dunning P, et al. Imaging cancer using PET: the effect of the bifunctional chelator on the biodistribution of a ^{64}Cu-labeled antibody. *Nucl Med Biol.* 2011;38:29–38.
26. Maier FC, Schmitt J, Maurer A, et al. Correlation between positron emission tomography and Cerenkov luminescence imaging in vivo and ex vivo using ^{64}Cu-labeled antibodies in a neuroblastoma mouse model. *Oncotarget.* 2016;7:67403–67411.
27. Dobrenkov K, Cheung NK. GD2-targeted immunotherapy and radioimmunotherapy. *Semin Oncol.* 2014;41:589–612.
28. Cheung NK, Kushner BH, Cheung IY, et al. Anti-G(D2) antibody treatment of minimal residual stage 4 neuroblastoma diagnosed at more than 1 year of age. *J Clin Oncol.* 1998;16:3053–3060.
29. Stabin MG. Uncertainties in internal dose calculations for radiopharmaceuticals. *J Nucl Med.* 2008;49:853–860.
30. Cheal SM, Xu H, Guo HF, et al. Theranostic pretargeted radioimmunotherapy of internalizing solid tumor antigens in human tumor xenografts in mice: curative treatment of HER2-positive breast carcinoma. *Theranostics.* 2018;8:5106–5125.